THE JOURNAL OF PHYSICAL CHEMISTRY B

Article

The Influence of Chain Rigidity and Dielectric Constant on the Glass Transition Temperature in Polymerized Ionic Liquids

Vera Bocharova, Zaneta Wojnarowska, Peng-Fei Cao, Yao Fu, Rajeev Kumar, Bingrui Li, Vladimir N Novikov, Sheng Zhao, Alexander M Kisliuk, Tomonori Saito, Jimmy W. Mays, Bobby G. Sumpter, and Alexei P. Sokolov

J. Phys. Chem. B, **Just Accepted Manuscript** • DOI: 10.1021/acs.jpcb.7b09423 • Publication Date (Web): 28 Nov 2017

The Influence of Chain Rigidity and Dielectric Constant on the Glass Transition Temperature in Polymerized Ionic Liquids

V. Bocharova[1*], Z. Wojnarowska[1,2,3], Peng-Fei Cao[1*], Y. Fu[4], R. Kumar[5,6], Bingrui Li,[1] V. N. Novikov[7], S. Zhao [7], A. Kisliuk[1], T. Saito[1], Jimmy W. Mays[1,7], B.G. Sumpter[5,6], A. P. Sokolov[1,7*]

[1]*Chemical Sciences Division, Oak Ridge National Laboratory, Oak Ridge, Tennessee 37831, USA*

[2] *Institute of Physics, University of Silesia, Uniwersytecka 4, 40-007 Katowice, Poland*

[3]*Silesian Center for Education and Interdisciplinary Research, 75 Pulku Piechoty 1A, 41-500 Chorzow, Poland*

[4]*Department of Aerospace Engineering & Engineering Mechanics, University of Cincinnati, Cincinnati, OH 45220*

[5]*Center for Nanophase Materials Sciences, Oak Ridge National Laboratory, Oak Ridge, Tennessee 37831, US*

[6]*Computational Sciences & Engineering Division, Oak Ridge National Laboratory, Oak Ridge, Tennessee 37831, USA*

[7]*Department of Chemistry, University of Tennessee, Knoxville, Tennessee 37996, USA*

Corresponding Authors

*E-mail: bocharovav@ornl.gov; caop@ornl.gov; sokolov@utk.edu

Abstract

Polymerized ionic liquids (PolyILs) are promising candidates for a wide range of technological applications due to their single ion conductivity and good mechanical properties. Tuning the glass transition temperature (T_g) in these materials constitutes a major strategy to improve room temperature conductivity while controlling their mechanical properties. In this work, we show experimental and simulation results demonstrating that in these materials T_g does not follow a universal scaling behavior with the volume of the structural units V_m (including monomer and counterion). Instead, T_g is significantly influenced by the chain flexibility and polymer dielectric

constant. We propose a simplified empirical model that includes the electrostatic interactions and chain flexibility to describe T_g in PolyILs. Our model enables design of new functional PolyILs with the desired T_g.

Introduction

Polymerized ionic liquids (PolyILs) are a relatively new class of materials that combines a high charge density of ionic liquids (ILs) with superior mechanical properties of polymers [1,2]. Due to a decreased mobility of one of the ions achieved by its chemical bonding to the polymer chain, PolyILs are essentially single ion conductors which facilitate their application in electrochemical devices [3,4,5]. One of the critical parameters for PolyILs, as for any other polymers, is the glass transition temperature, T_g. In polymers, T_g defines a transition from soft rubbery state to a "brittle" solid glassy state. Moreover, in case of PolyILs it also controls the room temperature ion conductivity. In general, a lower T_g provides for higher ion conductivity, σ, at ambient conditions [6,7,8]. Such correlation is achieved because conductivity is controlled by the rate of polymer segmental mobility at ambient temperature [9,10] which increases with decrease in T_g. Designing polymers with lower T_g is one of the traditional ways to achieve higher ion conductivity in polymer electrolytes[11,12]. Thus, understanding the dependence of T_g on chemical structure of PolyIL is critical for their design.

In earlier studies, it has been demonstrated that T_g in the imidazolium-based PolyILs scales well with the molecular volume of structural unit, V_m, (monomer plus counterion)[7,8]: T_g decreases with the increase in V_m. However, the physical origin of this behavior and whether such dependence holds for PolyILs of diverse chemical structures remain unknown. Similar behavior of T_g *vs* V_m has been reported for molecular ionic materials such as monomers of ionic liquids, ionic liquids, and inorganic salts[7, 13]. However, in spite of their ionic nature, the dependence of T_g on V_m in PolyILs and other ionic liquids doesn't collapse on a single master curve suggesting that there might be other structural factors controlling the glass transition. For instance, it is known that in polymers with prevailing van der Waals (vdW) interactions, the chain rigidity and side group bulkiness play an important role in affecting T_g[14,15]. However, the results from non-ionic polymers cannot be directly applied to polymers with prevailing electrostatic interactions, and therefore detailed studies are required to elucidate the role of different structural parameters on T_g behavior in these materials.

In this Letter, we analyze several PolyILs with different chemical structures, counterion sizes and charges, and chain rigidity (Figure 1). To unravel microscopic details, we also use coarse-grained molecular dynamics (MD) simulations. Our analysis clearly demonstrates that V_m is not the only parameter controlling T_g in PolyILs. The latter can change by a factor of two at the same V_m, depending on the polymer chain rigidity. To understand this dependence, we present a simple physical model that accounts for chain flexibility, electrostatic and vdW interactions. This model accurately describes the behavior of T_g *vs* V_m for PolyILs, their monomers, and ionic liquids, and unveils the importance of V_m, dielectric constant ε, and chain rigidity in controlling T_g of PolyILs.

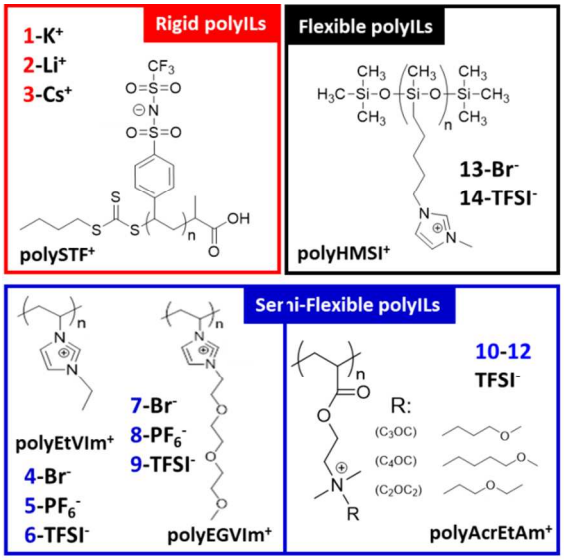

Figure 1. Chemical structures of PolyILs investigated in this paper.

Materials and Methods

1-vinyl imidazole was purchased from Alfa Aesar and distilled under vacuum prior to use. N,N-dimethylformamide (DMF, Alfa Aesar), 1-bromo-4-methoxy butane (C_4OC, Matrix Scientific), 1-bromo-3-methoxy propane (C_3OC, Matrix Scientific), 2-bromoethyl ethyl ether (C_2OC_2, Oakwood Chemical), bromoethane (Sigma Aldrich), diethylene glycol-2-bromoethyl methyl ether (TCI), lithium bis(trifluoromethanesulfonimide) (LiTFSI, Acros Organics), lithium hexafluorophosphate ($LiPF_6$, Alfa Aesar), dimethylformamide (DMF, anhydrous, Alfa Aesar), ethyl acetate (BDH), methanol (BDH), hexanes (BDH), tetrahydrofuran (THF, BDH) were used as received. Reversible Addition Fragmentation Chain Transfer Agent (RAFT-CTA) was

synthesized according to the previous reference[16]. Azobisisobutyronitrile (AIBN, Sigma-Aldrich) was recrystallized from ethanol prior to use. 2-(*Dimethylamino*) ethylacrylate (> 97%, TCI) was de-inhibited *via* passing through activated alumina column and inhibitor remover.

1. Synthesis of STF-based polyanions; PolyILs 1-3

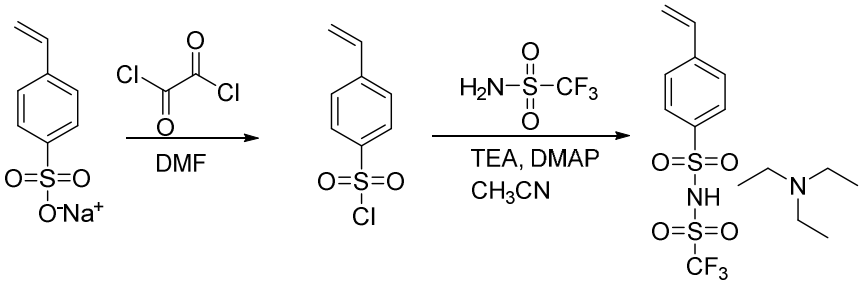

Scheme 1. Synthesis of (4-styrenesulfonyl)(trifluromethane-sulfonyl)imide triethylamine (STF-TEA)

Synthesis of 4-styrene sulfonyl chloride [17]: 8.8 g (43 mmol) of 4-styrenesulfonic acid sodium salt was slowly added to the thiolyl chloride (21.7 mL, 300 mmol) in a round bottom flask that was immersed in an ice bath. With magnetic stirring, the 12 mL dry DMF was added dropwise to the solution. The mixture was stirring at 0°C for 2 hours and ambient temperature for another 6 hours. The mixture was stay in the freezer overnight before it was poured into the ice water. The aqueous solution was extracted by diethyl ether for three times, and the combined organic layer was washed by water for additional two times. The organic solution was dried by Na_2SO_4, and after filtering, the ether solution was concentrated by rotary evaporation.

Synthesis of (4-styrenesulfonyl)(trifluromethane-sulfonyl)imide triethylamine (STF-TEA)[18]*:* The 4-styrene sulfonyl chloride (12.9g, 64 mmol) was dissolved in 20 mL of dried acetonitrile (CH_3CN) and placed in a three-neck round bottom flask that was immersed in an ice bath. 10 g trifluoromethylsulfonamide (68 mmol), 27 mL triethylamine (194 mmol) and 0.80 g (6.5 mmol) 4-dimethylaminopyridine was dissolved in 45 mL of dried CH_3CN, and the mixture was slowly added to the acetonitrile solution of the 4-styrene sulfonyl chloride *via* a dropping funnel. After two hours stirring in the ice bath, the mixture was stirred at room temperature for another 18 hours before the solvent was removed by rotary evaporation. The product was re-dissolved in 150 mL of dimethyl chloride (DCM), and the solution was washed by the aqueous solution of

$NaHCO_3$ (2%, 3×35mL), HCl (1mol/L, 4×30 mL). The ^{1}H NMR spectrum was shown in Figure S1 in Supplementary Information (SI).

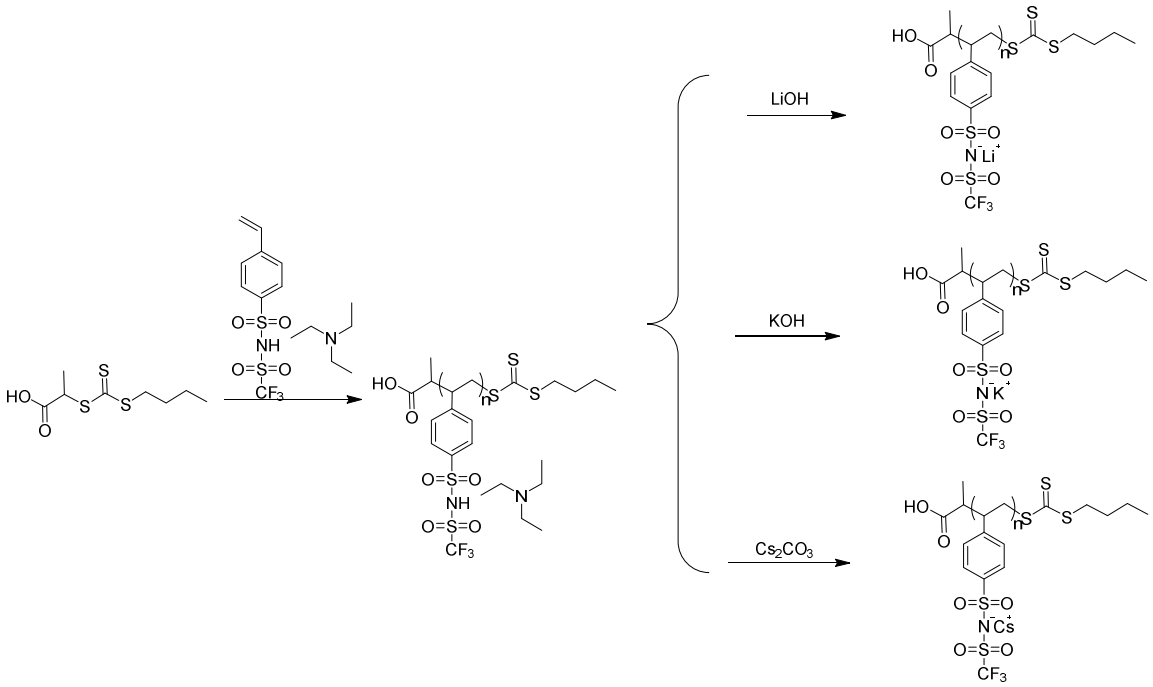

Scheme 2. Synthesis of poly(4-styrenesulfonyl)(trifluromethane-sulfonyl)imide with different counter ions

Synthesis of poly(4-styrenesulfonyl)(trifluromethane-sulfonyl)imide with different counter ions (*PolyILs 1-3)*: 119 mg (0.5 mmol) RAFT-CTA, 10.1g (25 mmol) STF-TEA and 8.2 mg (0.05 mmol) AIBN were dissolved in 50 mL dry dimethylformamide (DMF). After the solution in schedule tube was degassed for 30 min, the reaction was performed at 65 °C for 24 hours. The crude product was obtained by evaporating the solvent. The poly(STF-Li^+), poly(STF-K^+), and poly(STF-Cs^+) was obtained by adding excess LiOH, K_2CO3 and Cs_2CO_3 to the water/THF solution of the poly(STF-TEA) and stirring at 40 °C for 24 hours. The products were purified by dialysis against DI water/CH_3OH before further characterization. The typical ^{1}H NMR spectrum analysis was shown in Figure S2 of SI, and end group analysis suggested the DP_n of the

poly(STF-Li^+) is 116.08/4=29.02. The complete disappearance of the TEA signals after the couterion exchange (Figure S2 vs Figure S1) suggested the complete counter ion exchange.

M_n of poly(STF-Li^+) =322.22×29.02+238.38= 9,589 Da.

M_n of poly(STF-K^+) =354.38×29.02+238.38= 10,522 Da

M_n of poly(STF-Cs^{2+})=448.19×29.02+238.38= 13,244 Da

2. *Synthesis of poly(N-vinyl imidazole) based poly(ionic liquid)s; PolyILs 4-9.*

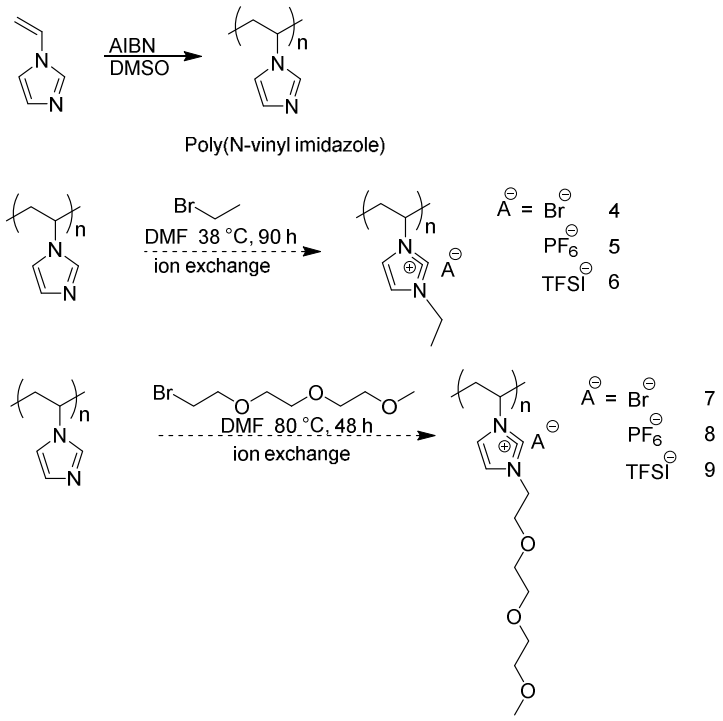

Scheme 3. Synthesis of poly(N-vinyl imidazole), poly(N-vinyl ethyl imidazolium), poly(N-vinyl diethylene glycol ethyl methyl ether imidazolium bromide)

Synthesis of Poly(N-vinyl imidazole): 1-vinyl imidazole (50 g, 0.531mol) and AIBN (0.1 mol%, 0.0872 g, 5.31×10^{-4} mol) dissolved in ~150 mL of DMF were charged into a round-bottomed flask equipped with a magnetic stirrer. The solution was purged with argon for 20 min and placed in an oil bath. The reaction proceeded at 65 °C for 17 h. The resulting reaction solution was precipitated into ethylacetate, re-dissolved in methanol, and re-precipitated into ethylacetate. The precipitation process was repeated 3 times. A resulting poly(N-vinyl imidazole) was white powder and dried under reduced pressure at 40°C overnight. The isolated yield was ~54%. Unfortunately, direct measurements of the molecular weight of PolyILs synthesized from this

precursor is very challenging and wasn't perform here, because it requires a combination of certain solvents to neutralize the charge of the polymer. According to previous reference[19], the reaction condition would afford the polymer with M_n of 42000 g/mol and PDI of 1.84. ^{1}H NMR (400 MHz, CD_3OD, δ): 1.8-2.3 (br,-C*H*$_2$CH-), 2.8-3.7 ppm (br, -CH$_2$C*H*-), 6.6-7.0 ppm (br, -NC*H*C*H*N-), 7.0-7.3 ppm (br, -NCHN-); here and below br stays for a broad peak in the NMR spectra.

Synthesis of poly(N-vinyl ethyl imidazolium, ***polyILs 4-6****)*: Poly(N-vinyl imidazole) (5 g) was dissolved in DMF (75 mL) in a round-bottomed flask equipped with a magnetic stirrer. Bromoethane (1.5 equivalent, 8.68 g, 5.95 mL) was charged into the reaction flask and the reaction proceeded at 38 °C for 90 h. Over the course of reaction, the solution became milky due to its low solubility of the product. The resulting reaction solution was precipitated into ethylacetate, redissolved in methanol, and reprecipitated into ethylacetate. The precipitation process was repeated 3 times. The resulting poly(N-vinyl ethyl imidazolium bromide) was dried under reduced pressure at 40°C overnight. Based on the chemical shift and integration in ^{1}H NMR spectrum, the conversion to imidazolium bromide was nearly quantitative, more than 96-97 %. ^{1}H NMR (400 MHz, CD_3OD, *δ*): 1.3-1.8 (br,-CH$_2$C*H*$_3$), 2.3-3.2 (br,-C*H*$_2$CH-), 4.1-4.4 (br,-C*H*$_2$CH$_3$), 4.5-4.7 ppm (br, -CH$_2$C*H*-), 7.3-8.2 ppm (br, -NC*H*C*H*N-), 9.1-9.8 ppm (br, -NC*H*N-)

TFSI exchange and PF_6 exchange were conducted in methanol with 1.5 equivalents of LiTFSI or $LiPF_6$, respectively. The product was precipitated into DI water, dissolved in acetone and precipitated into DI water. Precipitation and water rinsing were repeated several times.

Synthesis of poly(N-vinyl diethylene glycol ethyl methyl ether imidazolium, ***polyILs 7-9****):* Poly(N-vinyl imidazole) (1.77g) was dissolved in DMF (40 mL) in a round-bottomed flask equipped with a magnetic stirrer. Diethylene glycol-2-bromoethyl methyl ether (1.17 equivalent, 5 g) was charged into the reaction flask and the reaction proceeded at 80°C for 48 h. The resulting reaction solution was precipitated into ethylacetate, redissolved in methanol, and reprecipitated into ethylacetate. The precipitation process was repeated 3 times. The resulting poly(N-vinyl diethylene glycol ethyl methyl ether imidazolium bromide) was dried under reduced pressure at 40°C overnight. Based on the chemical shift and integration in the ^{1}H NMR, the conversion to imidazolium bromide was quantitative. ^{1}H NMR (400 MHz, CD_3OD, *δ*): 2.3-3.2 (br,-C*H*$_2$CH-),

3.4 (br,-OCH_3), 3.5-3.9 (br,-OCH_2CH_2O-), 3.9-4.1 (br,-NCH$_2$CH_2O-), 4.2-4.6 (br,-NCH_2CH$_2$O-), 4.6-4.8 ppm (br, -CH$_2$CH-), 7.3-8.2 ppm (br, -NCHCHN-), 9.0-9.8 ppm (br, -NCHN-)

TFSI and PF_6 exchange were conducted in methanol with 1.5 equivalents of LiTFSI and $LiPF_6$, respectively. The product was precipitated into DI water, redissolved in acetone and precipitated into DI water again. Precipitation and water rinsing were repeated several times. Similar PolyILs where oligomer of ethylene glycol was attached to the styrene type imidazolium-based monomer were reported earlier showing promising RT conductivity [20].

3. *Synthesis of poly(ammonium acrylate) based poly(ionic liquid)s: PolyILs 10-12.*

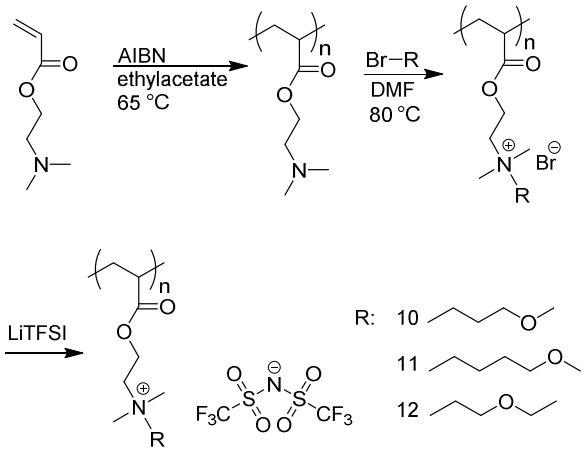

Scheme 4. Synthesis of poly(ammonium acrylate) based poly(ionic liquid)s: PolyILs 10-12

Synthesis of poly(2-(Dimethylamino) ethylacrylate): 2-(Dimethylamino) ethylacrylate (113 g, 120 mL) and AIBN (0.2 wt%, 226.3 mg) were dissolved in ethyl acetate (190 mL). Argon was bubbled through the solution for 20 min. The reaction proceeded for 5 h at 65 °C (Scheme 4). The resulting poly(dimethylamino ethylacrylate) was precipitated into hexanes for 5 times. The precipitated polymer was dried at 40 °C in vacuum for 24 h and the isolated yield was 52% (58 g). ^{1}H NMR (400 MHz, D_2O, δ) Poly(dimethylamino ethylacrylate): 1.3-2.0 ppm (br,-CH_2CH-), 2.1-2.2 ppm (br,-N(CH_3)$_2$), 2.2-2.4 ppm (br,-CH$_2$CH-), 2.4-2.8 ppm (br,-CH$_2$CH_2N(CH$_3$)$_2$), 3.8-4.3 ppm (br,-CH_2CH$_2$N(CH$_3$)$_2$).

Quaternization of poly(dimethylamino ethylacrylate): The reaction was performed *via* reaction with alkyl ether bromide (C_3OC, C_4OC, C_2OC_2). All the quaternization reactions were performed with 1.1 equimolar of alkyl ether bromide in anhydrous DMF at 80 °C for 24 h. The resulting quaternized poly(dimethylamino ethylacrylate) bromide was washed with THF several times.

The isolated polymer was dried at 40 °C in vacuum for 24 h. The synthesized quaternary ammonium bromide ionic liquid polymers include poly[(2-(acryloyloxy)ethyl)-N,N'-dimethyl-N-methoxy propyl-ammonium bromide] (C_3OC), poly[(2-(acryloyloxy)ethyl)-N,N'-dimethyl-N-methoxy butyl-ammonium bromide] (C_4OC), poly[(2-(acryloyloxy)ethyl)-N,N'-dimethyl-N-ethoxy ethyl-ammonium bromide] (C_2OC_2). ^{1}H NMR (400 MHz, D_2O, δ)**:** poly[(2-(acryloyloxy)ethyl)-N,N'-dimethyl-N-methoxy propyl-ammonium bromide], 1.5-2.0 ppm (2H, br, -C*H*$_2$CH-), 2.0-2.1 ppm (2H, br, -N(CH$_3$)$_2$CH$_2$C*H*$_2$CH$_2$OCH$_3$), 2.2-2.7 ppm (1H, br, -CH$_2$C*H*-), 3.0-3.2 ppm (6H, br, -N(C*H*$_3$)$_2$-), 3.2-3.3 ppm (3H, br, -N(CH$_3$)$_2$CH$_2$CH$_2$CH$_2$OC*H*$_3$), 3.3-3.6 ppm (4H, br, -N(CH$_3$)$_2$C*H*$_2$CH$_2$C*H*$_2$OCH$_3$), 3.6-3.8 ppm (2H, br, -OCH$_2$C*H*$_2$N(CH$_3$)$_2$-), 4.2-4.6 ppm (2H, br, -OC*H*$_2$CH$_2$N(CH$_3$)$_2$-); poly[(2-(acryloyloxy)ethyl)-N,N'-dimethyl-N-ethoxy ethyl-ammonium bromide], 0.9-1.4 ppm (3H, br, -N(CH$_3$)$_2$CH$_2$CH$_2$OCH$_2$C*H*$_3$), 1.5-2.0 ppm (2H, br, -C*H*$_2$CH-), 2.2-2.7 ppm (1H, br, -CH$_2$C*H*-), 3.0-3.3 ppm (6H, br, -N(C*H*$_3$)$_2$-), 3.4-3.6 ppm (2H, br, -N(CH$_3$)$_2$C*H*$_2$CH$_2$OCH$_2$CH$_3$), 3.6-3.7 ppm (2H, br, -N(CH$_3$)$_2$CH$_2$CH$_2$OC*H*$_2$CH$_3$), 3.7-3.8 ppm (2H, br, -OCH$_2$C*H*$_2$N(CH$_3$)$_2$-), 3.8-4.0 ppm (2H, br, -N(CH$_3$)$_2$CH$_2$C*H*$_2$OCH$_2$CH$_3$), 4.3-4.6 ppm (2H, br, -OC*H*$_2$CH$_2$N(CH$_3$)$_2$-)

Counter ion exchange: Ion exchange from bromide ion to bis(trifluoromethane)sulfonimide (TFSI) ion was performed using 1.2 equivalent of LiTFSI in water for 5 days (Scheme 4). The TFSI-exchanged ionic liquid polymers include poly[(2-(acryloyloxy)ethyl)-N,N'-dimethyl-N-methoxy propyl-ammonium TFSI] (C_3OC), poly[(2-(acryloyloxy)ethyl)-N,N'-dimethyl-N-methoxy butyl-ammonium TFSI] (C_4OC), poly[(2-(acryloyloxy)ethyl)-N,N'-dimethyl-N-ethoxy ethyl-ammonium TFSI] (C_2OC_2). Based on elemental analysis results detailed elsewhere [21] the content of Br in TFSI containing PolyILs doesn not exceed 1.6 %

4. Synthesis of poly(methylhydrosiloxane-graft-imidazolium); PolyILs 13, 14

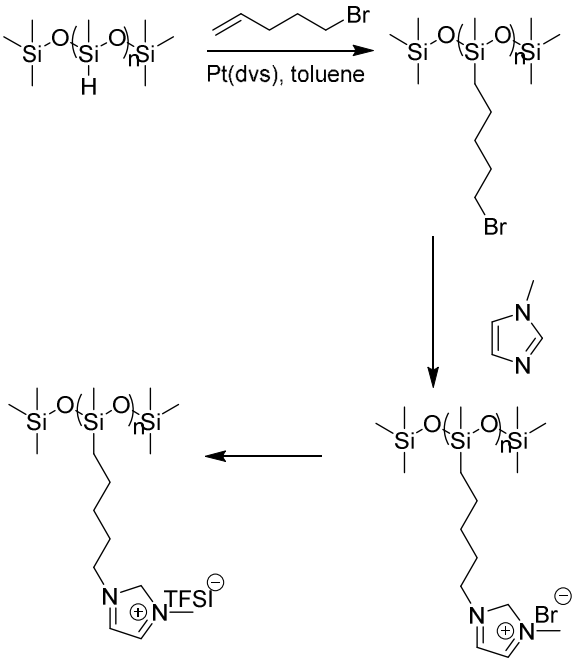

Scheme 5. Synthesis of poly(ammonium acrylate) based poly(ionic liquid)s: PolyILs 13,14.

*Synthesis of polymethylhydrosiloxane-graft-5-bromo-1-pentene (poly-MHS B5B)***:** To a pre-dried two neck round bottom flask equipped with a condenser, a rubber septum and a magnetic stirrer was added PMHS (2.0 g, 0.84 mmol) and B5B (5.0 g, 33.6 mmol, 40 eq) The reactor was purged with Ar for 20 min followed by the addition of a platinum-divinyltetramethyldisiloxane complex (Pt[dvs]) (30 μL). The reaction mixture was then stirred at 60 °C. The reaction progress was monitored using ^{1}H-NMR spectroscopy. Upon the completion of reaction, the solvent was removed and precipitated into excess methanol to obtain brown oil. Yield: 5.9 g, 98%. ^{1}H-NMR δ ($CDCl_3$, 500MHz): 3.41 (-C*H*$_2$-Br); 1.86 (-CH_2CH_2-Br); 1.28-1.53 (-CH_2CH_2-); 0.53 (Si-CH_2); 0.07 (Si-CH_3).

Synthesis of polymethylhydrosiloxane-graft-5-imidazolium-1-pentene bromide (poly-MHSImi Br, PolyIL 13). To a two neck round bottom flask equipped with a condenser and a magnetic stirrer was added the solution of PMHS-B5B (2.4 g, 0.36 mmol) in DCM (30 mL) and 1-methylimidazole (1.03 g, 12.5 mmol, 35 eq). The reaction was stirred at 70 °C for 72 h. Upon the completion of the reaction, the solvent was removed under reduced pressure and the product was recovered by washing with DCM three times and drying in vacuum oven at 40 °C. Yield: 3.2 g, 98%. ^{1}H-NMR δ (D_2O, 500MHz): 8.95 (NCHN); 7.56 (CH_3NC*H*C*H*N); 4.26 (NCH_2-); 3.95 (N-CH_3); 2.14-1.27 (4H, -CH_2-CH_2-); 0.58(Si-CH_2); 0.10 (Si-CH_3). Mass (ESI-) m/z: 78.92 (Br).

*Synthesis of polymethylhydrosiloxane-graft-5-imidazolium-1-pentene bis (trifluoromethane) sulfonamide (poly-MHSIm TFSI, PolyIL 14)***.** To a one neck round bottom flask equipped with a magnetic stirrer was added the solution of PMHS-Imi-Br (1.0 g, 0.11mmol) in deionized water DI-H_2O (20 mL) followed by the addition of LiTFSI (1.3 g, 6.9 mmol, 64 eq). The mixture was stirred at room temperature for 7 days. The precipitation was further washed with DI-H_2O 3 times and dried in vacuum oven at 40 °C. Yield: 1.5 g, 99%. ^{1}H-NMR δ (acetone-d_6, 500MHz): 8.87 (NCHN); 7.66 (CH_3NC*H*C*H*N); 4.30 (NCH_2-); 4.02 (N-CH_3); 2.03-1.30 (4H, -CH_2-CH_2-); 0.61 (Si-CH_2); 0.13 (Si-CH_3). Mass (ESI-) m/z: 180.89 (TFSI). The details of ion exchange are in [22].

Synthesis of monomers is described in SI.

Polymer Characterization:

Size exclusion chromatography (SEC) measurements were performed in THF/5% triethylamine mobile phase at 40 °C at flow rate of 1 mL/min using a Polymer Labs GPC-120 size exclusion chromatograph. The GPC-120 is equipped with Polymer Laboratories PL gel; 7.5mm x 300 mm (column size); 10 µm (particle size); 5,000 Å (pore size), a Precision Detector PD2040 (two angle static light scattering), Precision Detector PD2000DLS (dynamic light scattering), Viscotek 220 differential viscometer, and a Polymer Labs refractometer calibrated with narrow polydispersity polystyrene standards. The RI increment (d*n*/d*c*) was calculated online.

Elemental analysis for carbon, nitrogen, hydrogen, and sulfur were performed by Galbraith Laboratories, Inc. (Knoxville TN).

Differential Scanning Calorimetry (DSC) measurements were performed on TA Q2000. The samples were hermetically sealed in aluminum pans while using an empty pan for reference. These samples were initially equilibrated at 383 K for thirty minutes, then cooled down to 183 K and heated up to 453 K. The heating and cooling cycle was performed with a rate of 10K/min and repeated three times to make certain the reproducibility of the results. The glass transition temperature was estimated as the mid-point of the step in specific heat on cooling.

Measurements of density**:** The mass of the samples were measured using a weight balance (Mettler Toledo NewClassic MF Model MS105DU) with an accuracy of 0.01 mg. The gas pycnometer (Micromeretics Accupyc II 1340) measured the volume of penetrable helium gas within the sample and sample cup (total volume 0.1cm^3) until the pressure did not vary more

than 0.005psig/min during the equilibration period. The accuracy of the volume measurement is 0.0001 cm^3. This cycle was repeated 5 times for reproducibility. The density was then determined from the mass to volume ratio and the error of this measurement is less than 0.3%. All the density data were obtained at atmospheric pressure and at T = 20 °C. The molecular volume V_m was calculated based on the following equation $Vm = \frac{Mw}{\rho N_A}$, where M_w-molecular weight of the monomer and anion, ρ is the density, and N_A is the Avogadro constant.

Broadband Dielectric Spectroscopy (BDS) measurements of static dielectric constant: Dielectric measurements at ambient pressure from 10^{-1} to 10^6 Hz were carried out using a Novocontrol GMBH Alpha dielectric spectrometer. The sample was placed between two stainless steel electrodes of the capacitor with a gap of 0.1 mm. The dielectric spectra of PolyILs were collected over a wide temperature range. The temperature was controlled by the Novocontrol Quattro system, with the use of a nitrogen gas cryostat with a temperature stability of the samples of 0.1 K. The applied voltage was 0.1 V. The static dielectric constant was determined from fitting of the real part permittivity spectra at temperature above T_g using Havriliak-Negami[23] function. An example of fit is presented in the Fig. S3 in SI. The obtained values of the static dielectric constants of studied here PolyILs and monomers are presented in the Fig. S4 in SI.

Results & Discussion

Fourteen PolyILs with different backbones, side groups, and counterions of different charges and compositions [Fig.1 and Table 1] were synthesized in our lab and details of the synthesis are presented in[21,22], in the Materials and Methods section, and in the Supplementary Information (SI). Differential scanning calorimetry (DSC) was employed to estimate their glass transition temperature. Each sample was first cycled in the calorimeter to remove any prehistory, and then T_g was measured on cooling as the midpoint of the jump in the heat flow (Fig. 2). To calculate the molecular volume V_m of the PolyILs, the density was measured by pycnometry. The obtained values, including T_g, density and calculated molecular volume, are listed in the Table 1. In addition, we used T_g and V_m data for PolyILs, monomers, and ionic liquids reported in the literature[7, 8,13,24,25] (Figure 3). It is important to note that the major difference between ionic liquids and monomers lies in the presence of double bond in monomers which makes them polymerizable. To provide additional microscopic insight, we performed coarse-grained MD simulations using a bead-and-spring model with every forth bead having a charge. The radius of

the counterions was changed from 0.05 σ to 0.5 σ (σ is the bead diameter), so that the ratio of the counterion size to the chain bead size varies from 0.1 to 1. In addition, the dielectric constant and the chain rigidity were tuned in MD simulations. The T_g in MD simulations was estimated by the change in the slope of the specific volume with respect to temperature. Details of the simulations are presented in [26].

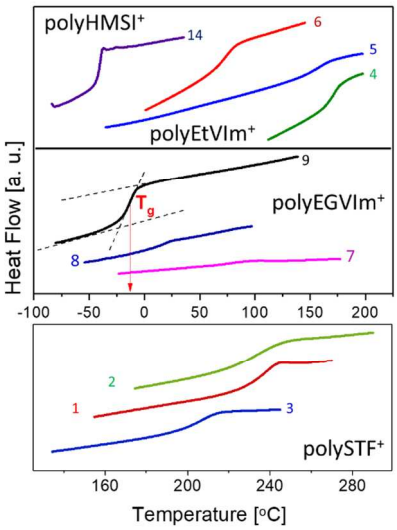

Figure 2. Representative thermograms of PolyILs studied in this work. T_g was obtained as a midpoint of the jump in heat flow.

Table 1. The physicochemical parameters of PolyILs studied herein, molecular weight, density, molecular volume, glass transition temperature.

No	PolyIL		M g/mol	ρ, g/cm^3	V_m nm^3	T_g K
	Cation	Anion				
		Rigid PolyILs				
1	K	polySTF	353.1	1.78	0.33	500
2	Li		320.94	1.60	0.33	507
3	Cs		446.9	2.33	0.31	470
		Semi-Flexible PolyILs				
4	polyEtVIm	Br	202.9	1.48	0.22	451
5		PF6	267.97	1.58	0.28	432
6		TFSI	403.15	1.61	0.41	344
7	polyEGVIm	Br	320.9	1.52	0.35	348
8		PF6	385.97	1.48	0.43	296
9		TFSI	521.15	1.53	0.56	261
10	polyAcrEtAm$^+$ C_2OC_2	TFSI	496	1.53	0.54	270
11	polyAcrEtAm$^+$		496	1.597	0.51	270

	C_3OC					
12	**polyAcrEtAm$^+$ C_4OC**		510	1.513	0.56	256
		Flexible PolyILs				
13	**polyHMSIm**	**TFSI**	491.15	1.48	0.55	233
14		**Br**	290.15	1.38	0.35	276
15	**I-EOT***		526	1.6	0.54	240
16	**I-AT***		508	1.37	0.61	249
17	**Poly Triazolium**	**TFSI****	879	1.5	0.97	211

T_g was determined by standard DSC measurements (10K/min);
***Data were taken from ref. [24];**
**** Data were taken from ref. [25] assuming density of 1.5 g/cm^3.**

The dependence of T_g on structural unit volume V_m shows a general behavior for polymerized ionic liquids and their monomers (Figure 3): T_g decreases with increase of V_m and starts to level off at V_m ~0.8-1nm^3. In the case of ionic liquids, T_g dependence goes through a clear minimum that is not that obvious for other systems (Fig. 3). Analysis of the data shows that V_m is not the only parameter controlling T_g in PolyILs because T_g can change by almost a factor of two at the same V_m. Flexible siloxane-based and phosphazene-based[24] PolyILs (open circles Fig.3) exhibit T_g comparable to that of monomers, while rigid polystyrene-based chains (open diamonds Fig.3) show significantly higher T_g at the same V_m (Fig. 3). This behavior is consistent with the known tendency in non-ionic polymers, where rigid chains show much higher T_g than the flexible ones [14,15,27,28,29].

The increase in T_g with increase in chain rigidity was also observed in our MD simulations (Fig. 4). Moreover, simulations also reveal the initial decrease in T_g with the increase in V_m, reaching a minimum and then leveling off at higher V_m. The $T_g(V_m)$ dependence remains qualitatively the same for different dielectric constant ε_s of the simulated polymer. However, an increase in ε_s results in suppression of T_g in both rigid and flexible chains. These MD results are very important because in experiment it is difficult to tune only dielectric constant without affecting other structural parameters of the polymer. The strong dependence of T_g on the dielectric constant emphasizes the importance of electrostatic interactions in PolyILs.

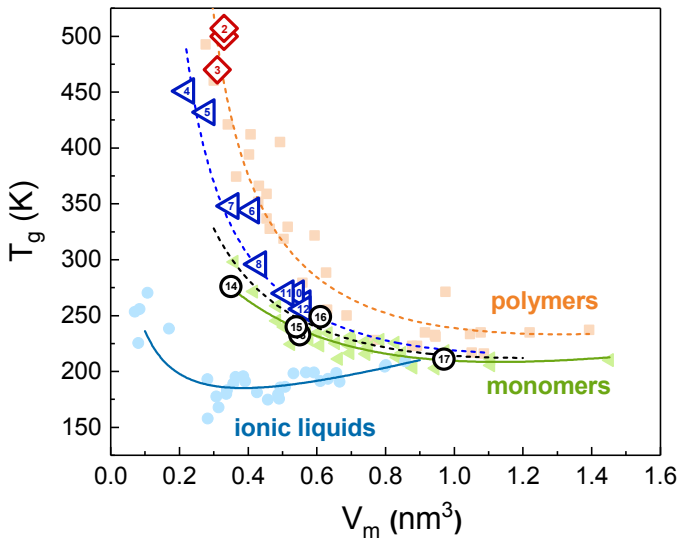

Figure 3 T_g as a function of molecular volume (monomer + counterion) for a number of PolyILs: open symbols present the data for PolyILs studied herein: open diamonds present rigid PolyILs, triangles for semi-flexible, and circles are for flexible PolyILs. The numbers in the open symbols correspond to the PolyILs in Table 1. Solid blue, green, orange symbols and open symbols 15-17 are literature data from [7,8,13] and [24,25], respectively. Solid lines are fits of the ionic liquids and monomers data to the Eq. (2). The fitting parameters for ionic liquids are A=-97±49 K, B=137±20 K·nm, and C=177±38 K/nm^2; and for monomers are A=-297±118 K, B=354±72 K·nm, and C=153±47 K/ nm^2. The dashed lines are curves calculated using the Eq. 4 with A, B, and C parameters of monomers while K were fixed to K=4 $\cdot 10^{-4}$, $2\cdot 10^{-4}$, and $1\cdot 10^{-4}$ nm^3/K for rigid (orange), semi-flexible (blue), and flexible (black) chains, respectively.

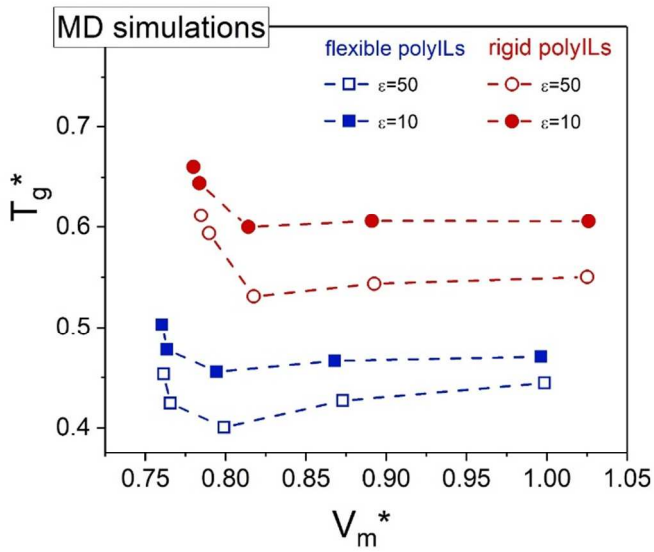

Figure 4. The results of MD simulations with two different values of the static dielectric constant ε_s. The asterisk on T_g and V_m means these quantities obtained from the MD simulations are in reduced Lennard-Jones units [26]. Figure was reproduced from [26].

To understand the observed behavior of T_g in PolyILs we note that the glass transition temperature usually correlates with the cohesive energy of the material[30,31]. There are two major contributions to the cohesive energy in ionic systems. The first one comes from electrostatic interactions of ions[32]. In a rough approximation, the electrostatic energy scales with the molecular volume V_m as

$$\boldsymbol{E_{el}} \propto \frac{\boldsymbol{e^2}}{\varepsilon_s \boldsymbol{V_m^{1/3}}} \quad (1)$$

Here e is the ion charge and $\boldsymbol{\varepsilon_s}$ is the static dielectric constant. The second contribution comes from the vdW interaction. For molecular van der Waals liquids, it was demonstrated experimentally that vdW interaction is roughly proportional to the surface area of the unit, $E_{vdW} \propto V_m^{2/3}$ [33]. As a result, the dependence of T_g on the molecular volume of structural units in ionic liquids can be approximated by the following expression:

$$\boldsymbol{T_{g0} = A + \frac{B}{V_m^{1/3}} + CV_m^{2/3}} \quad (2)$$

where $\boldsymbol{A}$, $\boldsymbol{B}$ and $\boldsymbol{C}$ are constants. In that case (Eq. 2), the electrostatic term dominates at small V_m leading to a sharp decrease in $T_g(V_m)$ with increasing V_m, while the vdW term should dominate

at larger V_m. This competition should lead to a broad minimum in $T_g(V_m)$. This minimum is indeed observed in the case of simple ionic liquids[13] (Fig. 3) where it was also explained by the competition between the electrostatic and Van der Waals forces. It should be noted that the term for vdW interaction used here is a result of empirical analysis of T_g behavior of simple vdW liquids and substantial theoretical work is required to understand the origin of this term. However, in spite of empirical nature of Eq.2 it describes $T_g(V_m)$ in ionic liquids and monomers (Fig. 3) quite well. The fitting revealed that the electrostatic term ($\boldsymbol{B}$) in the case of monomers is much stronger than in ionic liquids. This term is inversely proportional to the static dielectric constant ($\boldsymbol{i.e., B \propto \frac{1}{\varepsilon_s}}$), and the obtained difference in $\boldsymbol{B}$ suggests that ionic liquids has $\boldsymbol{\varepsilon_s}$ higher than the typical values obtained for monomers. Our analysis of the dielectric constant (Fig. S4 in SI) indeed confirms that on average $\boldsymbol{\varepsilon_s}$ in ionic liquids is higher than in monomers. It is important to note that monomers were specifically synthesized for these studies. Detailed description of monomer synthesis and structures are presented in the SI. In the present model, we neglected variation of $\boldsymbol{\varepsilon_s}$ for the same class of material. The fact that we were able to fit data for polymers, monomers, and ionic liquids with constant B suggests that variations of $\boldsymbol{\varepsilon_s}$ within each class are not very significant. Generally, it is possible to improve the model by adding $\boldsymbol{\varepsilon_s}$ as variable. However, it requires additional guidance from theory and further experimental validation.

It has been shown in [34] that T_g of a PolyIL increases with molecular weight (length of the chain) in a manner similar to usual vdW polymers [27, 29]. Thus to go from a monomer to a PolyIL we can use approximations developed for usual polymers. Among several ways to describe dependence of T_g on molecular weight (MW), we chose the Kanig-Ueberreiter equation [35]:

$$\frac{1}{T_g(MW)} = \frac{1}{T_{g\infty}} + \frac{D}{MW} \tag{3}$$

where $T_{g\infty}$ is the glass transition temperature at infinitely high MW, D is the coefficient that depends on the chain rigidity. This equation describes the dependence $T_g(MW)$ better than the Fox-Flory equation, especially at low MW [35]. We can invert eq. 3 and express the polymer $T_{g\infty}$ via monomer T_{g0}:

$$\frac{1}{T_{g\infty}} = \frac{1}{T_{g0}} - \frac{D}{M0} = \frac{1}{T_{g0}} - \frac{K}{V_m} = \left(A + \frac{B1}{\varepsilon_S V_m^{\frac{1}{3}}} + CV_m^{\frac{2}{3}}\right)^{-1} - \frac{K}{V_m} \tag{4}$$

where **M0** is the monomer mass, $\boldsymbol{K} = D/\rho$, and $\rho = M0/V_m$ is the monomer density. Here we introduced $B1 = B \cdot \boldsymbol{\varepsilon_s}$ to explicitly emphasize the dependence of T_g on the dielectric constant of the PolyILs. Assuming no strong dependence of density and dielectric constant on molecular weight, we can now predict the dependence of T_g on V_m in PolyILs (Fig. 3).

Figure 3 presents three different dashed curves calculated using the Eq.4 and $T_{g0}(V_m)$ for monomers (keeping parameters *A, B,* and *C* of the eq.2 the same) with only one adjustable parameter **K**. They describe the experimental data for PolyILs well, with the parameter **K** being the smallest for flexible (e.g. siloxane- and phosphazene-based) backbone and relatively large for rigid (e.g. polystyrene-based) chains. It is important to note that the flexibility parameters (**K)** obtained from this analysis are close to that of usual vdW polymers. For instance, the T_g(MW) data for polystyrene [27] gives for the parameter **K** ~0.001 [nm^3/K] (using V_m of polystyrene ~0.17 nm^3 and molecular weight of monomer 104 g/mol). This is about two times larger than **K** found for PolyILs with rigid chains (Fig. 3), but taking into account that K is found for different polymers in a broad range of V_m this is a reasonably good agreement. Thus the proposed model (eqs. 2, 4) provides a reasonable description of the V_m dependence of T_g in PolyILs. Given the fact that we could fit the data for the monomers and PolyILs using the same value of B, it is logical to suggest that there are no significant differences in their static dielectric constants. Indeed, the measured dielectric constants of monomers and PolyILs are very close (Fig S4). Obviously, explicit account for the difference in the static dielectric constant of various PolyILs could significantly improve the model description of their T_gs. However, the latter requires rigorous theory development. In contrast, we attempted to present a simplified qualitative picture of the role of chemical structure of PolyILs on their glass transition temperature that provides an excellent basis for further theoretical exploration.

Our analysis of the experimental and MD-simulations results revealed that in addition to V_m chain rigidity plays a significant role in defining T_g of PolyILs. However, from Fig 3 it also became apparent that by tuning V_m and chain flexibility it will be difficult to synthesize PolyILs with T_g below 200K since most of the monomers have T_g above this value (Fig. 3). This strongly limits the value of ionic conductivity that can be reached at ambient conditions. At the same time, our analysis (Fig. 3 and Fig. S4) shows that ionic liquids display a higher static dielectric constant than that of monomers, reflecting their overall lower T_g. As a consequence, strong

increase in the dielectric constant might be a promising route to drop T_g below 200K in PolyILs, especially at smaller V_m. In other words, only tuning the chain flexibility is not enough to significantly reduce T_g of PolyILs. Combination of polymer flexibility with high dielectric constant implemented into design of PolyILs may offer further lowering of T_g, providing high segmental and ion mobility at ambient temperature. An increase in the dielectric constant will also provide better ion dissociations, additionally improving ionic conductivity. However, further studies are required to ascertain similar behavior in other PolyILs. Another important alternative can be a decoupling of ion transport from segmental mobility[10,36,37,38,39,40,41,42,43,44]. It might provide significant enhancement of ion conductivity even at rather slow segmental dynamics of the polymer. However, this topic is out of scope of the current paper.

Conclusions

In conclusion, the presented detailed analysis of experimental and MD-simulations data revealed three important parameters controlling the glass transition temperature in PolyILs: chain rigidity, dielectric constant, and the size of the structural unit, V_m. To address the role of these parameters in determining T_g in PolyILs, we proposed a simplified empirical model that was shown to adequately describe the T_g *vs* V_m dependence of ionic liquids, monomers, and PolyILs. This model is important predictive tool that can help in design of PolyILs with a desired T_g. In particular, our results suggest that a strong increase in the dielectric constant of PolyILs is a promising direction for dropping T_g which can ultimately result in improved room temperature ion conductivity.

ASSOCIATED CONTENT

Supporting Information: The Supporting Information is available free of charge on the ACS Publications website at DOI: Monomer synthesis and structure (Scheme S1), ^{1}NMR spectra (Figure S1 and S2), Dielectric spectra (Figure S3), and Dielectric constants (Figure S4)

Acknowledgements

This work was supported by Laboratory Directed Research and Development program of Oak Ridge National Laboratory, managed by UT-Battelle, LLC, for the U.S. Department of Energy (DOE). APS, BGS, AK acknowledge partial financial support by the U.S. Department of Energy, Office of Science, Basic Energy Sciences, Materials Sciences and Engineering Division. MD simulations were performed at the Center for Nanophase Materials Sciences, which is a US DOE Office of Science User Facility. VNN thanks the NSF Polymer Program (DMR-1408811) for funding theoretical part. Z.W. is deeply grateful for the financial support by the National Science Centre within the framework of the Opus8 project (Grant DEC-2014/15/B/ST3/04246).

The Reference List

[1] Ohno, H.; Ito, K. Room-Temperature Molten Salt Polymers as a Matrix for Fast Ion Conduction. *Chem. Lett*. **1998**, *27*, 751−752.

[2] Yuan, J. Y.; Antonietti, M. Poly(Ionic Liquid)s: Polymers Expanding Classical Property Profiles. *Polymer* **2011**, *52*, 1469-1482.

[3] Tarascon, J.M.; Armand, M. Issues and Challenges Facing Rechargeable Lithium Batteries. *Nature* **2001**, *414*, 359-367.

[4] Meyer, W. H. Polymer Electrolytes for Lithium-Ion Batteries. *Adv. Mater*. **1998**, *10*, 439-448.

[5] Palacín, M.R. Recent Advances in Rechargeable Battery Materials: a Chemist's Perspective. *Chem. Soc. Rev.*, **2009**, *38*, 2565–2575.

[6] Ohno, H. Electrochemical Aspects of Ionic Liquids ISBN: 978-0-471-76252-2.

[7] Choi, U. H.; Mittal, A.; Price Jr, T. L.; Lee, M.; Gibsonb, H.W.; Runt, J.; Colby R. H. Molecular Volume Effects on the Dynamics of Polymerized Ionic Liquids and their Monomers. *Electrochimica Acta*, **2015**, *175*, 55-61.

[8] Choi, U. H.; Ye, Y. S.; de la Cruz, D. S.; Liu, W. J.; Winey, K. I.; Elabd, Y. A.; Runt, J.; Colby, R. H. Dielectric and Viscoelastic Responses of Imidazolium-Based Ionomers with Different Counterions and Side Chain Lengths. *Macromolecules* **2014**, *47*, 777-790.

[9] Ratner, M. A.; Shriver, D. F.; Ion Transport in Solvent-Free Polymers. *Chem. Rev*., **1988** , *88*, 109 − 124.

[10] Angell, C.A. Fast Ion Motion in Glassy and Amorphous Materials. *Solid State Ionics* **1983**, *9–10*, 3-16.

[11] Fan, F.; Wang Y.; Sokolov A. P. Ionic Transport, Microphase Separation, and Polymer Relaxation in Poly(Propylene Glycol) and Lithium Perchlorate Mixtures. *Macromolecules*, **2013**, *46*, 9380–9389.

[12] Obadia, M.M.; Jourdain, A.; Serghei, A.; Ikeda, T.; Drockenmuller, E. Cationic and Dicationic 1,2,3-Triazolium-Based Poly(Ethylene Glycol Ionic Liquid)s. *Polym. Chem*., **2017**, *8*, 910-917.

[13] Xu, W.; Cooper, E.I.; Angell, C.A. Ionic Liquids: Ion Mobilities, Glass Temperatures, and Fragilities. *J. Phys. Chem. B* **2003**, *107*, 6170-6178.
[14] Ngai, K. L.; Roland, C. M. Chemical Structure and Intermolecular Cooperativity: Dielectric Relaxation Results. *Macromolecules* **1993**, *26*, 6824–6830.
[15] Kunal, K.; Robertson, C.G.; Pawlus, S.; Hahn, S. F.; Sokolov, A. P. Role of Chemical Structure in Fragility of Polymers: a Qualitative Picture. *Macromolecules,* **2008**, *41*, 7232-7238.
[16] Lim, J; Yang, H.; Paek, K.; Cho, C.-H.; Kim, S.; Bang, J.; Kim, B. J "Click" Synthesis of Thermally Stable Au Nanoparticles with Highly Grafted Polymer Shell and Control of Their Behavior in Polymer Matrix. *J. Polym. Sci. Part A Polym. Chem*. **2011**, *49*, 3464-3474.
[17] Ishizone, T.; Tsuchiya, J.; Hirao, A.; Nakahama, S. Anionic Polymerization of Monomers Containing Functional Groups. 4. Anionic Living Polymerization of N,N-Dialkyl-4-Vinylbenzenesulfonamides. *Macromolecules* **1992,** *25*, 4840-4847.
[18] Meziane, R.; Bonnet, J.-P.; Courty, M.; Djellab, K.; Armand, M. Single-Ion Polymer Electrolytes Based on a Delocalized Polyanion for Lithium Batteries. *Electrochim. Acta* **2011,** *57*, 14-19.
[19] Green, M. D.; Salas-de la Cruz, D.; Ye, Y.; Layman, J. M.; Elabd, Y. A.; Winey, K. I.; Long, T. E. Alkyl-Substituted N-Vinylimidazolium Polymerized Ionic Liquids: Thermal Properties and Ionic Conductivities. *Macro. Chem. Phys.,* **2011**, *212*, 2522-2528.
[20] Jia, Z. ; Yuan, W.; Sheng, C.; Zhao, H.; Hu, H. ; Baker G. L. Optimizing the Electrochemical Performance of Imidazolium-Based Polymeric Ionic Liquids by Varying Tethering Groups. *J. Polym. Sci. A* **2015**, *53*, 1339–1350.
[21] Fan, F.; Wang, Y.; Hong, T.; Heres, M. F.; Saito, T.; Sokolov, A. P. Ion Conduction in Polymerized Ionic Liquids with Different Pendant Groups. *Macromolecules*, **2015**, *48*, 4461–4470.
[22] Wojnarowska , Z.; Feng, H.; Fu, Y.; Cheng, S.; Carroll, B.; Kumar, R.; Novikov, V. N.; Kisliuk, A. M.; Saito, T.; Kang, N.-G.; et al. Effect of Chain Rigidity on the Decoupling of Ion Motion from Segmental Relaxation in Polymerized Ionic Liquids: Ambient and Elevated Pressure Studies. *Macromolecules*, **2017**, *50*, 6710–6721.
[23] Havriliak, S.; Negami, S. A Complex Plane Representation of Dielectric and Mechanical Relaxation Processes in Some Polymers. *Polymer* **1967**, *8*, 161–210.
[24] Bartels, J.; Hess, A.; Shiau, H-S.; Allcock, H.R.; Colby, R-H.; Runt, J. Synthesis, Morphology, and Ion Conduction of Polyphosphazene Ammonium Iodide Ionomers. *Macromolecules*, **2015**, *48*, 111−118.
[25] Jourdain, A.; Serghei, A.; Drockenmuller, E. Enhanced Ionic Conductivity of a 1,2,3-Triazolium-Based Poly(Siloxane Ionic Liquid) Homopolymer. *ACSMacroLett*., **2016**, *5*, 1283−1286.
[26] Fu, Y.; Bocharova, V.; Ma, M.; Sokolov, A.P.; Sumpter, B. G.; Kumar, R. Effects of Counterion Size and Backbone Rigidity on Dynamics of Ionic Polymer Melts and Glasses. *Phys. Chem. Chem. Phys*., **2017**, *19*, 27442-27451.
[27] Santangelo, P.G.; Roland, C.M. Molecular Weight Dependence of Fragility in Polystyrene. *Macromolecules* **1998**, *31*, 4581-4585.

[28] Ding, Y.; Novikov, V. N.; Sokolov, A. P.; Calliaux, A.; Dalle-Ferrier, C.; Alba-Simionesco, C.; Frick, B. Influence of Molecular Weight on Fast Dynamics and Fragility of Polymers. *Macromolecules* **2004**, *37*, 9264-9272.

[29] Hintermeyer, J.; Herrmann, A.; Kahlau, R.; Goiceanu, C.; Rössler, E. A. Molecular Weight Dependence of Glassy Dynamics in Linear Polymers Revisited. *Macromolecules* **2008**, *41*, 9335-9344.

[30] Barton, A. F. M. *CRC Handbook of Polymer-Liquid Interaction Parameters and Solubility Parameters* CRC Press, Boca Raton, 1990.

[31] Bicerano, J. *Prediction of Polymer Properties* CRC Press, Boca Raton, 2002.

[32] Eisenberg, A.; Farb, H.; Cool, L. G. Glass Transitions in Ionic Polymers. *J. Polym. Sci*., Part A-2 **1966**, *4*, 855-868.

[33] Novikov, V.N.; Rössler, E.A. Correlation Between Glass Transition Temperature and Molecular Mass in Non-Polymeric and Polymer Glass Formers. *Polymer* **2013**, *54*, 6987-6991.

[34] Fan, F.; Wang, W.; Holt, A. P.; Feng, H.; Uhrig, D.; Lu, X.; Hong, T.; Wang, Y.; Kang, N.-G.; Mays, J.; Sokolov, A.P. Effect of Molecular Weight on the Ion Transport Mechanism in Polymerized Ionic Liquids. *Macromolecules* **2016**, *49*, 4557−4570.

[35] Ueberreiter, K.; Kanig, G. Self-Plasticization of Polymers. *J. Colloid Sci*., **1952**, *7*, 569-583.

[36] Wang, Y.; Fan, F.; Agapov, A.L.; Yu, X.; Hong, K.; Mays, J.; Sokolov, A.P. Design of Superionic Polymers—New Insights from Walden Plot Analysis. *Solid State Ionics* **2014**, *262*, 782–784.

[37] Wang, Y.; Fan, F.; Agapov, A.L.; Saito, T.; Yang, J.; Yu, X.; Hong, K.; Mays, J.; Sokolov, A.P. Examination of the Fundamental Relation Between Ionic Transport and Segmental Relaxation in Polymer Electrolytes. *Polymer* **2014**, *55*, 4067-4076.

[38] Imrie, T.; Ingram, M.D.; McHattie, G.S. Ion Transport in Glassy Polymer Electrolytes. *J. Phys. Chem. B*, **1999**, *103*, 4132–4138.

[39] Ueno, K.; Angell, C.A. On the Decoupling of Relaxation Modes in a Molecular Liquid Caused by Isothermal Introduction of 2 nm Structural Inhomogeneities *J. Phys. Chem. B*, **2011**, *115*, 13994–13999.

[40] Agapov, A.L.; Sokolov, A.P. Decoupling Ionic Conductivity from Structural Relaxation: A Way to Solid Polymer Electrolytes? *Macromolecules* **2011,** *44*, 4410 –4414.

[41] Wang, Y.; Agapov, A.L.; Fan, F.; Hong, K.; Yu, X.; Mays, J.; Sokolov, A. P. Decoupling of Ionic Transport from Segmental Relaxation in Polymer Electrolytes. *Phys. Rev. Lett*. **2012**, *108*, 088303-088308.

[42] Sasabe, H.; Saito, S. Relationship Between Ionic Mobility and Segmental Mobility in Polymers in the Liquid State. *Polym. J.* (Tokyo), **1972**, *3*, 624-630.

[43] Wojnarowska, Z.; Paluch, Z. Recent Progress on Dielectric Properties of Protic Ionic Liquids. *Journal of Physics: Condensed Matter* **2015**, *27*, 073202-073222.

[44] Ingram, M.D.; Imrie, C.T. New Insights from Variable-Temperature and Variable-Pressure Studies into Coupling and Decoupling Processes for Ion Transport in Polymer Electrolytes and Glasses. *Solid State Ionics* **2011**, *196*, 9-17.

TOC Graphic

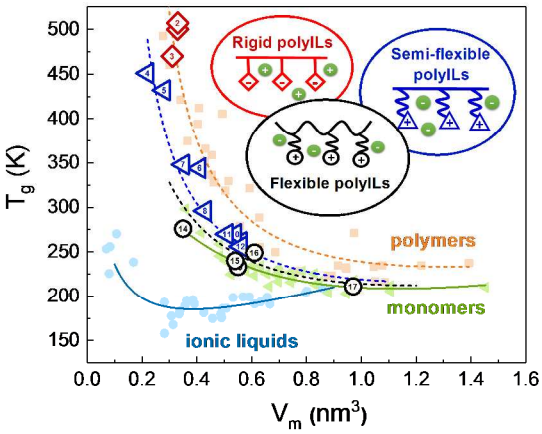
Rigid polyILs
Semi-flexible polyILs
Flexible polyILs
polymers
monomers
ionic liquids
T_g (K)
V_m (nm^3)
500
450
400
350
300
250
200
150
0.0
0.2
0.4
0.6
0.8
1.0
1.2
1.4
1.6